Enhanced Apoptotic Reaction Correlates with Suppressed Tumor Glucose Utilization After Cytotoxic Chemotherapy: Use of ^{99m}Tc-Annexin V, ^{18}F-FDG, and Histologic Evaluation

Toshiki Takei, MD[1]; Yuji Kuge, PhD[2]; Songji Zhao, MD[2]; Masayuki Sato, BS[3]; H. William Strauss, MD[4]; Francis G. Blankenberg, MD[5]; Jonathan F. Tait, MD, PhD[6]; and Nagara Tamaki, MD[1]

[1]Department of Nuclear Medicine, Graduate School of Medicine, Hokkaido University, Sapporo, Japan; [2]Department of Tracer Kinetics, Graduate School of Medicine, Hokkaido University, Sapporo, Japan; [3]Department of Radiopharmaceutical Chemistry, Health Sciences University of Hokkaido, Tobetsu, Japan; [4]Department of Nuclear Medicine, Memorial Sloan–Kettering Cancer Center, New York, New York; [5]Division of Nuclear Medicine, Department of Radiology, Stanford University School of Medicine, Stanford, California; and [6]Department of Laboratory Medicine, University of Washington, Seattle, Washington

Cancer chemotherapy enhances the apoptosis, whereas apoptosis is a suicidal mechanism requiring energy. We determined the relationship between apoptosis and glucose utilization during cancer chemotherapy using ^{99m}Tc-annexin V (^{99m}Tc-annexin A5) and ^{18}F-FDG and compared their uptake with histologic findings in a rat tumor model. **Methods:** Allogenic hepatoma cells (KDH-8) were inoculated into the left calf muscle of male Wistar rats (WKA). Eleven days after the inoculation, the rats were randomly divided into 3 groups: The first group ($n = 7$) received a single dose of gemcitabine (90 mg/kg, intravenously), the second group ($n = 8$) received cyclophosphamide (150 mg/kg, intraperitoneally), and the third group ($n = 7$) was untreated and served as the control group. We injected ^{99m}Tc-annexin V 48 h after the chemotherapy and then injected ^{18}F-FDG to all rats 1 h before sacrifice. Six hours after ^{99m}Tc-annexin V injection, the rats were sacrificed and the organs, including the tumor, were removed and radioactivity was counted. The radioactivities of ^{18}F and ^{99m}Tc in the organs were determined using normalization by tissue weight. Histologic evaluation by the terminal deoxynucleotidyl transferase-mediated deoxyuridine triphosphate nick-end labeling (TUNEL) method and the immunostaining of glucose transporter-1 (GLUT-1) were also performed to obtain the indices of apoptosis and glucose utilization, respectively. The rate of positively stained cells was calculated and analyzed statistically. **Results:** After chemotherapy using gemcitabine and cyclophosphamide, the ^{99m}Tc-annexin V uptake (percentage injected dose per gram × kg [(%ID/g) × kg]; mean ± SD) in tumor increased significantly (0.062 ± 0.012 (%ID/g) × kg in the gemcitabine-treated group and 0.050 ± 0.012 (%ID/g) × kg in the cyclophosphamide group vs. 0.031 ± 0.005 (%ID/g) × kg in the control group; $P < 0.01$). In contrast, the ^{18}F-FDG in tumor decreased significantly (0.483 ± 0.118 (%ID/g) × kg in the gemcitabine group and 0.583 ± 0.142 (%ID/g) × kg in the cyclophosphamide group) compared with that in the control group (0.743 ± 0.084 (%ID/g) × kg; $P < 0.01$). In addition, ^{18}F-FDG uptake in tumor negatively correlated with ^{99m}Tc-annexin V uptake ($r = -0.75$; $P < 0.01$). In the gemcitabine and cyclophosphamide groups, the rate of TUNEL positively stained cells was significantly higher than that in the control group (10.2% ± 1.7% and 8.0% ± 1.5% vs. 5.2% ± 1.5%; $P < 0.01$), whereas the GLUT-1 expression level showed no definite changes in histologic analyses. **Conclusion:** These data indicate that an enhanced apoptotic reaction correlated with suppressed tumor glucose utilization after cytotoxic chemotherapy as determined using radiotracers and histologic evaluation. The increase in ^{99m}Tc-annexin V and the decrease in ^{18}F-FDG in tumor can be useful markers for predicting therapeutic outcomes and for prognosis at the early stage of chemotherapy.

Key Words: molecular imaging; ^{18}F-FDG; ^{99m}Tc-annexin V; apoptosis; cancer chemotherapy

J Nucl Med 2005; 46:794–799

Apoptosis, or programmed cell death, is activated in the course of successful antineoplastic therapy (*1–3*). Determining baseline levels of apoptosis and the increment of apoptosis induced by therapy can serve as useful prognostic markers (*4,5*). Cancer chemotherapy with agents such as 2′,2′-difluoro-2′-deoxycytidine (gemcitabine) and cyclophosphamide not only arrest metabolism and induce DNA alkylation, respectively, but also enhance apoptosis (*6,7*). Early in the course of apoptosis, phosphatidylserine (PS) is expressed on the external leaflet of the cell membrane. Annexin V (annexin A5), a human protein with a high affinity for membrane-bound PS, can be labeled with ^{99m}Tc for in vivo imaging of apoptosis (*8*). In an earlier study, we used this imaging technique to quantify the time course and

Received Sep. 11, 2004; revision accepted Dec. 8, 2004.

For correspondence or reprints contact: Nagara Tamaki, MD, Department of Nuclear Medicine, Graduate School of Medicine, Hokkaido, University, Kita 15 Nishi 7, Kita-ku, Sapporo 060-8638, Japan.

E-mail: natamaki@med.hokudai.ac.jp

intensity of apoptosis induced by treatment with cyclophosphamide (*7,9,10*).

Because apoptosis requires energy to destroy cellular DNA and produce apoptosomes, evaluating cellular metabolism in the course of apoptosis may identify the process with an increase in substrate consumption. Since glucose is a major substrate for tumor cells, serial images recorded with the glucose analog ^{18}F-FDG may be useful for this purpose. Although ^{18}F-FDG PET is widely applied for clinical staging, differential diagnosis, therapy monitoring, detecting recurrence, and prognostic prediction of malignant diseases (*11,12*), clinical studies typically demonstrate a decrease in ^{18}F-FDG uptake before morphologic regression after appropriate chemotherapeutic regimens. Furthermore, the degree of initial metabolic suppression by chemotherapy can be correlated with the therapeutic outcomes such as malignant lymphoma or head and neck cancer (*13,14*).

This study was undertaken to compare the apoptotic response with the metabolic response in animals with implanted hepatomas and to determine the relative sensitivity of each approach to identify successful treatment.

MATERIALS AND METHODS

Preparation of Animal Models

All procedures involving animals were performed in accordance with institutional guidelines (Guide for the Care and Use of Laboratory Animals of Hokkaido University). KDH-8 is a rat transplantable hepatocellular carcinoma induced by 3′-methyl-4-dimethylaminoazobenzene in Wistar King Aptekman/Hok (WKA/H) rats (supplied by the Experimental Animal Institute, Graduate School of Medicine, Hokkaido University, Sapporo) and maintained in vivo by intraperitoneal passage every 5 d (supplied by the Department of Pathologic Oncology, Graduate School of Medicine, Hokkaido University, Sapporo). KDH-8 rat allogenic hepatoma cells (1×10^6 cells per rat) were inoculated into the left calf muscle of 8-wk-old male WKA/H rats (*7,15*). No obvious rejection or graft-versus-host reaction was observed. Our previous study showed a high uptake of ^{18}F-FDG and high expression of GLUT-1 in this KDH-8 rat tumor (*16*). Cyclophosphamide (Endoxan; Baxter) and gemcitabine (GEMZAR; Eli Lilly) were each dissolved in saline for injection. Eleven days after the intramuscular injection of KDH-8 tumor cells, rats, which weighed 187–253 g (measuring about 15 mm in diameter), with palpable tumors were randomly divided into 3 groups. The first group ($n = 7$) was treated with a single dose of gemcitabine (90 mg/kg, intravenously), the second group ($n = 8$) was treated with a single dose of cyclophosphamide (150 mg/kg, intraperitoneally), and the third group ($n = 7$) was untreated (control group) (*7,17*). All rats were anesthetized with pentobarbital (0.025 mg/kg, intraperitoneally) when these treatments were undertaken.

Methods Using Radioactive Tracers and Determining Biodistribution

Human annexin V was produced by expression in *Escherichia coli* as described (*8,18–21*). Annexin V was derivatized with hydrazinonicotinamide (HYNIC) and then labeled with ^{99m}Tc with tricine as coligand as described (*8*) to a specific activity of 3.0 MBq/μg protein. Rats were fasted overnight before sacrifice. ^{99m}Tc-Annexin V (37 MBq) was injected intravenously approximately 48 h after chemotherapy. The animals were under pentobarbital anesthesia at the time of radiopharmaceutical injection. One hour before sacrifice, 20 MBq of ^{18}F-FDG were injected intravenously. The radiopharmaceuticals were injected intravenously into the coccygeal vein. The blood sugar level was measured immediately before ^{18}F-FDG injection (BS1) and immediately before sacrifice (BS2). Six hours after the ^{99m}Tc-annexin V injection (1 h after ^{18}F-FDG injection), the rats were sacrificed by whole-blood sampling under ether inhalation anesthesia. The tumor, an aliquot of blood, and the contralateral femoral muscle were removed, cleaned, and weighed; radioactivity was determined using an automatic γ-counter (1480 WIZARDTM3″; Wallac Co., Ltd.). First, ^{18}F activity was measured (energy peak, 511 keV ± 20%). After >24 h for decay of ^{18}F, ^{99m}Tc activity was determined (energy peak, 140 keV ± 20%). A time-line diagram of this study is shown in Figure 1.

Activity in each window was compared with an aliquot of the injected dose to permit calculation of percentage uptake/gram of tissue after normalization to the rat's weight ((%ID/g) × kg). The tumor samples were divided into 3 parts. Using aliquots of the tumor tissues, formalin-fixed, paraffin-embedded specimens then were prepared for subsequent histologic studies. The tumor-to-muscle ratio (T/M ratio) and the tumor-to-blood ratio (T/B ratio) were calculated from the (%ID/g) × kg value in each tissue (*7,10,15*).

Histologic Evaluation

Apoptotic cells were determined by hematoxylin and eosin staining and the direct immunoperoxidase detection of digoxigenin-labeled 3′ DNA strand breaks by the use of the terminal deoxynucleotidyl transferase-mediated deoxyuridine triphosphate nick-end labeling (TUNEL) method. The formalin-fixed, paraffin-embedded tissues were sectioned at 3-μm thickness. TUNEL was performed according to a standard procedure using a commercially available kit (Apoptosis in situ Detection Kit; Wako Pure Chemical Industries, Ltd.).

The expression of glucose transporter-1 (GLUT-1) in adjacent slices was examined according to a standard immunostaining

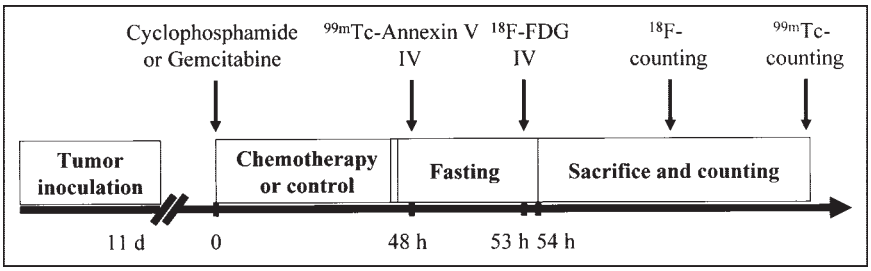

FIGURE 1. Time-line diagram of this study. IV = intravenously.

procedure. Deparaffinized sections were incubated with an anti–GLUT-1 antibody (Chemicon International, Inc.) at 37°C. The bound antibody was visualized using the avidin/biotin conjugate immunoperoxidase procedure with a HISTOFINE SAB-PO kit (Nichirei) and 3,3′-diaminobenzine tetrahydrochloride.

TUNEL and GLUT-1 positively stained cells were counted in 10 randomly selected high-power (×200) fields (with no knowledge of the treatment to avoid experimental bias) (*7,10,15*). The rate of TUNEL positively stained cells was determined by calculating the average percentage. The expression level of GLUT-1 was assessed semiquantitatively by the product of scores estimated (intensity × % positivity) according to our previous reports (*16,22*). The intensity of staining was graded (intensity) from 0 to 3 (0, not stained; 1, equivocal; 2, intense staining; and 3, very intense staining) and the percentage of positively stained cells (% positivity) was scored from 1 to 5 (1, 0%–20%; 2, 21%–40%; 3, 41%–60%; 4, 61%–80%; and 5, 81%–100%). The mean values of these levels were determined as immunohistologic GLUT-1 expression level.

Statistical Analysis

All values are shown as mean ± SD. Statistical analyses were performed using an unpaired Student *t* test to evaluate the significance of differences in values between the control and treated rats (*7,10*). Simple regression analysis was performed to compare the uptake of ^{99m}Tc-annexin V and that of ^{18}F-FDG. A 2-tailed value of $P < 0.05$ was considered significant.

RESULTS

Determination of Apoptosis

The uptake of ^{99m}Tc-annexin V in tumor tissue after gemcitabine and cyclophosphamide treatment was 0.062 ± 0.012 and 0.050 ± 0.012 (%ID/g) × kg, respectively (Table 1). The uptake of ^{99m}Tc-annexin V in tumor in both treated groups was significantly higher than that in the control group (0.031 ± 0.005 (%ID/g) × kg; $P < 0.01$). Two of the radiopharmaceuticals' uptakes in blood and muscle were not altered significantly by the 2 kinds of chemotherapeutic treatments. The TBRs of ^{99m}Tc-annexin V were 2.021 ± 0.323, 2.482 ± 0.407, and 1.414 ± 0.082 and the TMRs of ^{99m}Tc-annexin V were 7.283 ± 1.632, 7.095 ± 1.328, and 4.497 ± 0.824 in the gemcitabine-treated, cyclophosphamide-treated, and control groups, respectively. Both TBR and TMR in the treated groups were also significantly higher than those in the control group ($P < 0.01$).

In the gemcitabine-treated, cyclophosphamide-treated, and control groups, the rate of TUNEL positively stained cells were 10.2% ± 1.7%, 8.0% ± 1.5%, and 5.2% ± 1.5%, respectively. These apoptotic rates also increased in both treatment groups (Table 1).

Determination of Glucose Utilization

The uptake of ^{18}F-FDG in tumor tissue after gemcitabine and cyclophosphamide treatment was 0.483 ± 0.118 and 0.583 ± 0.142 (%ID/g) × kg, respectively (Table 2). The uptake of ^{18}F-FDG in tumor in both treated groups was significantly lower than that in the control group (0.743 ± 0.084 (%ID/g) × kg; $P < 0.01$). The TBRs of ^{18}F-FDG were 9.885 ± 4.592, 12.21 ± 7.145, and 15.21 ± 1.487 and the TMRs of ^{18}F-FDG were 15.15 ± 6.062, 7.859 ± 4.464, and 33.44 ± 4.721 in the gemcitabine-treated, cyclophosphamide-treated, and control groups, respectively. Both the TBRs and TMRs in the treated groups were also significantly lower than those in the control group ($P < 0.05$).

The expression levels of GLUT-1 estimated on the basis of positivity (intensity × percentage) were 58.3 ± 4.9, 61.1 ± 6.9, and 60.5 ± 5.6 in the gemcitabine-treated, cyclophosphamide-treated, and control groups, respectively. Although all 3 groups showed very high expression levels in the cancer cells, there was no statistically significant difference in the expression level of GLUT-1 between treated and control tissues (Table 2).

Relationship Between Uptake of ^{99m}Tc-Annexin V and ^{18}F-FDG in Tumor

Figure 2 shows a scattergram of the uptake of ^{99m}Tc-annexin V and ^{18}F-FDG in tumor. ^{18}F-FDG uptake in tumor showed a significantly negative correlation with that of ^{99m}Tc-annexin V uptake ($r = -0.75$; $P < 0.01$).

Blood Glucose Level and Tumor Weight

The tumor weights were 3.239 ± 1.520, 4.168 ± 2.007, and 3.503 ± 1.145 g in the gemcitabine-treated, cyclophosphamide-treated, and control groups, respectively. The blood glucose levels at BS1 was 114.1 ± 13.01, 118.9 ±

TABLE 1
Apoptotic Indices According to Uptake of ^{99m}Tc-Annexin V and Rate of TUNEL Positively Stained Cells

Parameter	Control	Gemcitabine	Cyclophosphamide
Tumor uptake (%ID/g) × kg	0.031 ± 0.005	0.062 ± 0.012*	0.050 ± 0.012*
Blood uptake (%ID/g) × kg	0.022 ± 0.002	0.024 ± 0.004*	0.025 ± 0.004*
Muscle uptake (%ID/g) × kg	0.007 ± 0.002	0.007 ± 0.003*	0.009 ± 0.002*
T/B ratio	1.414 ± 0.082	2.021 ± 0.323*	2.482 ± 0.407*
T/M ratio	4.497 ± 0.824	7.283 ± 1.632*	7.095 ± 1.328*
TUNEL positive (%)	5.2 ± 1.5	10.2 ± 1.7*	8.0 ± 1.5*

*$P < 0.01$ compared with control group.
Data are mean ± SD.

TABLE 2
Tumor Glucose Metabolic Markers According to Uptake of ^{18}F-FDG and Index of GLUT-1 Positivity

Parameter	Control	Gemcitabine	Cyclophosphamide
Tumor uptake (%ID/g) × kg	0.743 ± 0.084	0.483 ± 0.118*	0.583 ± 0.142*
Blood uptake (%ID/g) × kg	0.048 ± 0.005	0.045 ± 0.011*	0.036 ± 0.007*
Muscle uptake (%ID/g) × kg	0.022 ± 0.002	0.021 ± 0.004*	0.026 ± 0.006*
T/B ratio	15.21 ± 1.487	9.885 ± 4.592*	12.21 ± 7.145*
T/M ratio	33.44 ± 4.721	15.15 ± 6.062*	7.859 ± 4.464*
GLUT-1 (intensity × %)	60.5 ± 5.6	58.3 ± 4.9	61.1 ± 6.9

*$P < 0.01$ compared with control group.
Data are mean ± SD.

12.29, and 117.3 ± 5.283 mg/dL and those at BS2 were 93.86 ± 13.45, 94.14 ± 14.70, and 91.86 ± 14.86 mg/dL in the gemcitabine-treated, cyclophosphamide-treated, and control groups, respectively. Both tumor weight and blood glucose level in all groups did not change significantly after chemotherapeutic treatment with gemcitabine and cyclophosphamide (Table 3).

DISCUSSION

This study demonstrated that tumor glucose utilization declined after a single dose of gemcitabine or cyclophosphamide, which was not based on reduced GLUT-1 expression. This decline in glucose utilization occurred at a time of increased apoptosis. These molecular events occurred before the actual tumor regression. These data suggest that apoptosis induced by chemotherapy is not always accompanied by glucose hypermetabolism for survival reactions as previously reported (*17,23*).

In clinical oncology, the decrease in ^{18}F-FDG uptake was usually associated with a good lesion response, especially in malignant lymphoma, esophageal cancer, and head and neck cancer (*13,14*). Recently, there have been reports that

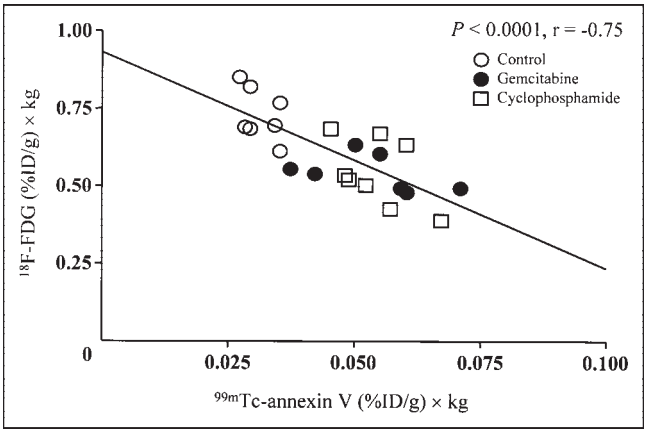

FIGURE 2. Negative correlation between ^{18}F-FDG uptake and ^{99m}Tc-annexin V uptake in control, gemcitabine-treated, and cyclophosphamide-treated groups. ^{18}F-FDG uptake ((%ID/g) × kg) = 0.932 − (6.956 ^{99m}Tc-annexin V uptake ((%ID/g) × kg)) ($r = -0.75$; $P < 0.01$).

^{99m}Tc-annexin V is very useful for detecting and in vivo imaging of apoptosis (*4,24,25*). The present study demonstrated that induction of apoptosis with a single dose of chemotherapy was associated with a striking reduction in ^{18}F-FDG uptake and a modest increase in annexin localization. Although appropriate chemotherapy induces metabolic regression (reflected by a reduction in ^{18}F-FDG uptake) before morphologic change of cancer tissue, the basic mechanism underlying the decrease in glucose uptake is not well understood. We observed that the uptake of ^{18}F-FDG was definitely decreased to approximately 55% of the control value by both gemcitabine and cyclophosphamide before the actual tumor regression. Both gemcitabine and cyclophosphamide themselves rarely affected blood glucose level, and our present results confirmed this observation. Mazurek et al. (*26,27*) suggested the following mechanisms: Chemotherapeutic agents damage DNA and then they activate adenosine diphosphate ribosyl transferase to repair DNA for proliferation. Because this repair requires a great amount of energy, intracellular nicotinamide adenine dinucleotide, which is an electron carrier, and adenosine triphosphate, which is required in intracellular phosphorylation, are so exhausted by anaerobic hyperglycolysis, they cannot compensate. This intracellular "famine" may depress important glycolytic enzymes. Consequently, glucose uptake in cancer cells decreases as a result of these intracellular reactions.

The relationship between apoptosis and glucose utilization at the early stage of cancer chemotherapy is also controversial (*17,28*). Haberkorn et al. reported an increase in glucose (^{18}F-FDG) uptake early after chemotherapy using gemcitabine for Morris hepatoma and interpreted it as a stress reaction of cancer cells as a protective mechanism against apoptosis (*17*). This interpretation may be reasonable since a great amount of energy is required for DNA repair. Furthermore, DNA damage promotes apoptosis via other pathways, such as the activation of tumor-suppression gene (e.g., p53) and inhibition of antiapoptotic molecules (e.g., Fas and phosphatidylinositol 3-phosphate kinase (PI3K-Akt)) (*29–32*). Activated caspases also have an essential role in the series of apoptosis. As a result of these

TABLE 3
Blood Glucose Level and Weight of Whole Body and Tumor

Parameter	Control	Gemcitabine	Cyclophosphamide	*P*
BS1 (mg/dL)	117.3 ± 5.283	114.1 ± 13.01	118.9 ± 12.29	ns
BS2 (mg/dL)	91.86 ± 14.86	93.86 ± 13.45	94.14 ± 14.70	ns
Whole-body weight (g)	209.6 ± 14.59	215.4 ± 14.29	204.9 ± 14.86	ns
Tumor weight (g)	3.503 ± 1.145	3.239 ± 1.520	4.168 ± 2.007	ns

ns = not significant.
Data are mean ± SD.

molecular interactions, an irreversible DNA-laddering reaction occurs at the end of programmed cell death. Because this reaction must use energy, glucose demand may increase temporarily. Occasionally, a "metabolic flare" was often observed on ^{18}F-FDG PET images after hormonal therapy was administrated for estrogen receptor–positive human breast cancer. This phenomenon may indicate responsiveness (*33*). Here, we speculated that tumor glucose hypometabolism was finally superior to the energy demand. Previous studies demonstrated maximal apoptosis 1 or 2 d after chemotherapy (*7,10,34*). Although ATP depletion and decrease in glucose uptake occur as apoptosis progresses after chemotherapy, these 2 phenomena themselves were reported to promote apoptosis (*26,35*). Thus, we confidently assumed that tumor glucose utilization after chemotherapy increasingly becomes hypometabolic and, finally, irreversible. Additionally, Spaepen et al. suggested that FDG uptake mainly correlates with the viable tumor cell fraction for 15-d monitoring of tumor response using a leukemia model in mice with severe combined immunodeficiency (*36*). However, changes in glucose metabolism by chemotherapy still remain to be clarified. Correlation between tumor uptake of ^{18}F-FDG and ^{99m}Tc-annexin V may help clarify the significance of early glucose utilization changes in clinical oncology. A long-time course of chemotherapeutic effects should also be evaluated in vivo models. Cremerius et al. reported FDG PET must be performed 2 wk after completion of therapy of metastatic germ cell tumor (*37*). Until the various histologic changes that influence glucose utilization become inactive, a high accuracy of FDG PET evaluation cannot be maintained. The serial ^{18}F-FDG and ^{99m}Tc-annexin V images each provide useful data for predicting a therapeutic response.

In this study, we investigated whether GLUT-1 expression affects tumor glucose utilization. However, GLUT-1 protein expression level did not change significantly after chemotherapy in our immunohistologic analyses. Histologic GLUT-1 overexpression correlated significantly with tumor characterization and prognosis in many cancer tissues. If ^{18}F-FDG uptake is high, GLUT-1 expression level also tends to be high. These findings are usually seen more with malignant lesions (*38*). In the present study, GLUT-1 expression was evaluated with "percent positive" and "intensity" per randomly selected high-power microscopic field. However, changes in cellularity by chemotherapy may affect the values of GLUT-1 expression rate if it is normalized to the cell number. Further evaluation considering the cellularity is needed to confirm the present results, although no apparent difference in the cell numbers (approximately 1,000 cells per field) was observed among the 3 groups. Unfortunately, little was known in our study as to why GLUT-1 positivity was not seemingly altered by chemotherapy. Using MR spectroscopy and western blotting, Rivenzon-Segal et al. suggested that glycolysis and GLUT-1 expression in breast tumor cells were positively correlated at both estrogen stimulation and tamoxifen inhibition (*39*). We deduce 2 points: (a) GLUT-1 protein expression is maintained for self-survival and (b) there is a time lag between the present protein expression on the cell surface and messenger RNA expression. Furthermore, this mechanism is more complicated because of the participation in hexokinase or the other GLUTs. Cyclophosphamide treatment was reported to modify tumor glycolytic rate and increase the intracellular lactate concentration in RIF-1 tumor (*40*).

In the present study, the animals were anesthetized with pentobarbital, which is known to depress glucose metabolism. This kind of barbiturate is a sedative-hypnotic drug, and its high lipophilicity has a direct effect on the central nervous system. The depressed glucose metabolism by pentobarbital may cause systemic errors. On the other hand, direct competition between FDG and blood glucose is regarded as the cause of impaired FDG uptake in tumors. Accordingly, we used anesthetized animals to avoid any physiologic variations, including blood glucose concentration, among the groups. It is also well known that blood glucose concentration is easily affected by any stress in awake animals.

The weakness of our study is the acute or chronic nature of our measurements. The animals received a single, high dose of chemotherapy to treat a rapidly growing tumor. The tumor response was evaluated within hours of chemotherapy administration. Whether serial administration of more moderate doses could produce a similar early result cannot be determined from the present study. However, there are clinical instances when an early indication of therapeutic

response is required. This is particularly necessary when toxic chemotherapy is used in tumors, such as gastric or lung cancer, where the response rate is around 50%. In those cases, an indication of nonresponse would permit a rapid redirection of therapy to other agents.

CONCLUSION

We found that the enhanced apoptotic reaction correlated with suppressed tumor glucose utilization after cytotoxic chemotherapy. The imaging results were confirmed by histologic evaluation. The decrease in tumor glucose utilization was independent of GLUT-1 overexpression. The increase in ^{99m}Tc-annexin V uptake in tumor as well as the decrease in ^{18}F-FDG uptake can be useful markers for predicting therapeutic outcomes and for prognosis at the early stage of chemotherapy.

ACKNOWLEDGMENTS

The authors are grateful to Professors Shinzo Nishi, Kazuo Miyasaka, and Koh-ichi Seki of the Central Institute of Isotope Science, Hokkaido University, for supporting this work. The authors also thank Koutaro Suzuki, Hidenori Katsuura, Hidehiko Omote, Hiroshi Arai, Keiichi Magota, and Miho Nakajima of the Facility of Radiology, Hokkaido University Medical Hospital, for assistance; Theseus Imaging Corp. for providing annexin V protein; and Makoto Sato, Sumitomo Heavy Industries, Ltd., for ^{18}F-FDG syntheses.

REFERENCES

1. Kerr JF, Wyllie AH, Currie AR. Apoptosis: a basic biological phenomenon with wide-ranging implications in tissue kinetics. *Br J Cancer.* 1972;26:239–257.
2. Thompson CB. Apoptosis in the pathogenesis and treatment of disease. *Science.* 1995;267:1456–1462.
3. Joseph B, Lewensohn R, Zhivotovsky B. Role of apoptosis in the response of lung carcinomas to anti-cancer treatment. *Ann NY Acad Sci.* 2000;926:204–216.
4. Belhocine T, Steinmetz N, Green A, Rigo P. In vivo imaging of chemotherapy-induced apoptosis in human cancers. *Ann NY Acad Sci.* 2003;1010:525–529.
5. Vermeersch H, Ham H, Rottey S, et al. Intraobserver, interobserver, and day-to-day reproducibility of quantitative ^{99m}Tc-HYNIC annexin-V imaging in head and neck carcinoma. *Cancer Biother Radiopharm.* 2004;19:205–210.
6. Ng SSW, Tsao MS, Chow S, Hedley DW. Inhibition of phosphatidylinositide 3-kinase enhances gemcitabine-induced apoptosis in human pancreatic cancer cells. *Cancer Res.* 2000;60:5451–5455.
7. Mochizuki T, Kuge Y, Zhao S, et al. Detection of apoptotic tumor response in vivo after a single dose of chemotherapy with ^{99m}Tc-annexin V. *J Nucl Med.* 2003;44:92–97.
8. Blankenberg FG, Katsikis PD, Tait JF, et al. In vivo detection and imaging of phosphatidylserine expression during programmed cell death. *Proc Natl Acad Sci USA.* 1998;95:6349–6354.
9. Kuge Y, Sato M, Zhao S, et al. Feasibility of ^{99m}Tc-annexin V for repetitive detection of apoptotic tumor response to chemotherapy: an experimental study using a rat tumor model. *J Nucl Med.* 2004;45:309–312.
10. Takei T, Kuge Y, Zhao S, et al. Time course of apoptotic tumor response following a single dose of chemotherapy: comparison with ^{99m}Tc-annexin V uptake and histologic findings in an experimental model. *J Nucl Med.* 2004;45:2083–2087.
11. Cohade C, Wahl RL. PET scanning and measuring the impact of treatment. *Cancer J.* 2002;8:119–134.
12. Rohren EM, Turkington TG, Coleman RE. Clinical applications of PET in oncology. *Radiology.* 2004;231:305–332.
13. Brun E, Kjellen E, Tennvall J, et al. FDG PET studies during treatment: prediction of therapy outcome in head and neck squamous cell carcinoma. *Head Neck.* 2002;24:127–135.
14. Spaepen K, Stroobants S, Verhoef G, Mortelmans L. Positron emission tomography with [^{18}F]FDG for therapy response monitoring in lymphoma patients. *Eur J Nucl Med Mol Imaging.* 2003;30(suppl 1):S97–S105.
15. Zhao S, Kuge Y, Tsukamoto E, et al. Effects of insulin and glucose loading on FDG uptake in experimental malignant tumours and inflammatory lesions. *Eur J Nucl Med.* 2001;28:730–735.
16. Mochizuki T, Tsukamoto E, Kuge Y, et al. FDG uptake and glucose transporter subtype expressions in experimental tumor and inflammation models. *J Nucl Med.* 2001;42:1551–1555.
17. Haberkorn U, Bellemann ME, Brix G, et al. Apoptosis and changes in glucose transport early after treatment of Morris hepatoma with gemcitabine. *Eur J Nucl Med.* 2001;28:418–425.
18. Wood BL, Gibson DF, Tait JF. Increased erythrocyte phosphatidylserine exposure in sickle cell disease: flow-cytometric measurement and clinical associations. *Blood.* 1996;88:1873–1880.
19. Tait JF, Smith C. Site-specific mutagenesis of annexin V: role of residues from Arg-200 to Lys-207 in phospholipid binding. *Arch Biochem Biophys.* 1991;288:141–144.
20. Tait JF, Engelhardt S, Smith C, Fujikawa K. Prourokinase-annexin V chimeras: construction, expression, and characterization of recombinant proteins. *J Biol Chem.* 1995;270:21594–21599.
21. Tait JF, Brown DS, Gibson DF, Blankenberg FG, Strauss HW. Development and characterization of annexin V mutants with endogenous chelation sites for ^{99m}Tc. *Bioconjug Chem.* 2000;11:918–925.
22. Zhao S, Kuge Y, Tsukamoto E, et al. Fluorodeoxyglucose uptake and glucose transporter expression in experimental inflammatory lesions and malignant tumours: effects of insulin and glucose loading. *Nucl Med Commun.* 2002;23:545–550.
23. Haberkorn U, Bellemann ME, Altmann A, et al. PET 2-fluoro-2-deoxyglucose uptake in rat prostate adenocarcinoma during chemotherapy with gemcitabine. *J Nucl Med.* 1997;38:1215–1221.
24. Belhocine T, Steinmetz N, Hustinx R, et al. Increased uptake of the apoptosis-imaging agent ^{99m}Tc recombinant human annexin V in human tumors after one course of chemotherapy as a predictor of tumor response and patient prognosis. *Clin Cancer Res.* 2002;8:2766–2774.
25. van de Wiele C, Lahorte C, Vermeersch H, et al. Quantitative tumor apoptosis imaging using technetium-99m-HYNIC annexin V single photon emission computed tomography. *J Clin Oncol.* 2003;21:3483–3487.
26. Mazurek S, Boschek CB, Eigenbrodt E. The role of phosphometabolites in cell proliferation, energy metabolism, and tumor therapy. *J Bioenerg Biomembr.* 1997;29:315–330.
27. Mazurek S, Eigenbrodt E. The tumor metabolome. *Anticancer Res.* 2003;23:1149–1154.
28. Moley KH, Mueckler MM. Glucose transport and apoptosis. *Apoptosis.* 2000;5:99–105.
29. Fresno Vara JA, Casado E, de Castro J, et al. PI3K/Akt signalling pathway and cancer. *Cancer Treat Rev.* 2004;30:193–204.
30. Raff M. Cell suicide for beginners. *Nature.* 1998;396:119–122.
31. Thorburn A, Thorburn J, Frankel AE. Induction of apoptosis by tumor cell-targeted toxins. *Apoptosis.* 2004;9:19–25.
32. Sellers WR, Fisher DE. Apoptosis and cancer drug targeting. *J Clin Invest.* 1999;104:1655–1661.
33. Mortimer JE, Dehdashti F, Siegel BA, et al. Metabolic flare: indicator of hormone responsiveness in advanced breast cancer. *J Clin Oncol.* 2001;19:2797–2803.
34. Blankenberg FG, Naumovski L, Tait JF, Post AM, Strauss HW. Imaging cyclophosphamide-induced intramedullary apoptosis in rats using ^{99m}Tc-radiolabeled annexin V. *J Nucl Med.* 2001;42:309–316.
35. Bacurau RF, O'Toole CE, Newsholme P, Costa Rosa LF. Sub-lethal concentrations of activated complement increase rat lymphocyte glutamine utilization and oxidation while lethal concentrations cause death by a mechanism involving ATP depletion. *Cell Biochem Funct.* 2002;20:183–190.
36. Spaepen K, Stroobants S, Dupont P, et al. [^{18}F]FDG PET monitoring of tumour response to chemotherapy: does [^{18}F]FDG uptake correlate with the viable tumour cell fraction? *Eur J Nucl Med Mol Imaging.* 2003;30:682–688.
37. Cremerius U, Effert PJ, Adam G, et al. FDG PET for detection and therapy control of metastatic germ cell tumor. *J Nucl Med.* 1998;39:815–822.
38. Medina RA, Owen GI. Glucose transporters: expression, regulation and cancer. *Biol Res.* 2002;35:9–26.
39. Rivenzon-Segal D, Boldin-Adamsky S, Seger D, Seger R, Degani H. Glycolysis and glucose transporter 1 as markers of response to hormonal therapy in breast cancer. *Int J Cancer.* 2003;107:177–182.
40. Poptani H, Bansal N, Jenkins WT, et al. Cyclophosphamide treatment modifies tumor oxygenation and glycolytic rates of RIF-1 tumors: ^{13}C magnetic resonance spectroscopy, Eppendorf electrode, and redox scanning. *Cancer Res.* 2003;63:8813–8820.